



Etoricoxib prevents progression of osteolysis in repeated intra-articular monosodium urate-induced gouty arthritis in rats

Yen-You Lin^{a,1}, Yen-Hsuan Jean^{b,1}, Sung-Chun Lin^b, Chien-Wei Feng^c, Hsiao-Mei Kuo^d, Yu-Cheng Lai^{e,f},
Tsu-Jen Kuo^{e,g}, Nan-Fu Chen^h, Hsin-Pai Lee^{b,*}, Zhi-Hong Wen^{e,i,*}

^a Department of Sports Medicine, China Medical University, No. 91 Hsueh-Shih Road, Taichung 40402, Taiwan

^b Department of Orthopedic Surgery, Pingtung Christian Hospital, Pingtung, No. 60, Dalian Road, Pingtung 90059, Taiwan

^c Department of Obstetrics and Gynecology, Kaohsiung Medical University Hospital, Kaohsiung Medical University, No.100, Tzyou 1st Rd., Sanmin Dist., Kaohsiung City 80756, Taiwan

^d Center for Neuroscience, National Sun Yat-sen University, No.70, Lianhai Road, Gushan District, Kaohsiung 80424, Taiwan

^e Department of Marine Biotechnology and Resources, National Sun Yat-Sen University, No.70, Lianhai Road, Gushan District, Kaohsiung 80424, Taiwan

^f Department of Orthopedics, Kaohsiung Veterans General Hospital, No.386, Dazhong 1st Road, Zuoying District, Kaohsiung 81362, Taiwan

^g Department of Stomatology, Kaohsiung Veterans General Hospital, No.386, Dazhong 1st Road, Zuoying District, Kaohsiung 81362, Taiwan

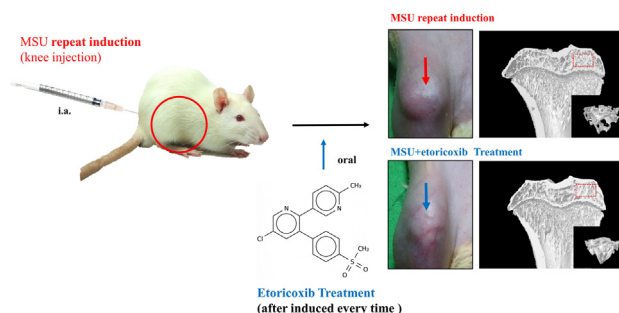
^h Division of Neurosurgery, Department of Surgery, Kaohsiung Armed Forces General Hospital, #2, Zhongzheng 1st Road, Lingya District, Kaohsiung 802, Taiwan

ⁱ Institute of BioPharmaceutical Sciences, National Sun Yat-sen University, No.70, Lianhai Road, Gushan District, Kaohsiung 80424, Taiwan

HIGHLIGHTS

- The chronic and repeated gouty arthritis (GA) could be induced by repeated-injection of monosodium urate (MSU) in the joints of rats.
- The repeated attacks of MSU-induced chronic GA significantly produced osteoclast activated protein expression, osteolysis and cartilage degeneration.
- NSAID, etoricoxib not only attenuated nociception but also played a protective role on cartilage in chronic and repeated attacks of GA.
- NSAID, etoricoxib could attenuate the chronic and repeated gouty-induced osteoclastogenesis.

GRAPHICAL ABSTRACT



ARTICLE INFO

Article history:

Received 20 November 2019

Revised 23 February 2020

Accepted 25 February 2020

Available online 29 February 2020

Keywords:

Chronic, recurrent gouty arthritis

Rat model

Osteoclastogenesis

Micro-CT

ABSTRACT

Deposition of monosodium urate (MSU) crystals in the joint or synovium is the major factor in Gouty arthritis (GA). The clinical features of chronic and recurrent GA include pain and the subsequent development of chronic tophaceous GA with multiple tophi deposits accompanied by osteolysis. The majority of previous animal studies have focused on MSU-induced acute GA without making observations regarding osteolysis. In the study, intra-articular injections of MSU into the knee (2 times/week for 10 weeks) was used to induce chronic and recurrent attacks of GA that in turn induced progressive osteolysis. Moreover, we also evaluated whether the clinical, nonsteroidal anti-inflammatory drug (NSAID) etoricoxib attenuated the osteoclastogenesis of progressive osteolysis. The knee morphometry and the expression of osteoclastogenesis-related proteins (cathepsin K and matrix metalloproteinase-9 and -13) in the knee were examined by micro-CT and immunohistochemistry, respectively. Results showed that oral etoricoxib not only significantly attenuated the nociceptive behaviors of the rats but that it also inhibited

Peer review under responsibility of Cairo University.

* Corresponding authors at: Department of Marine Biotechnology and Resources, National Sun Yat-Sen University, Kaohsiung, Taiwan (Z.-H. Wen).

E-mail addresses: hplee0929@gmail.com (H.-P. Lee), wzh@mail.nsysu.edu.tw (Z.-H. Wen).

¹ These authors contributed equally to this work.

<https://doi.org/10.1016/j.jare.2020.02.014>

2090-1232/© 2020 THE AUTHORS. Published by Elsevier BV on behalf of Cairo University.

This is an open access article under the CC BY-NC-ND license (<http://creativecommons.org/licenses/by-nc-nd/4.0/>).

the expression of osteoclastogenesis-related proteins in their knee joints in chronic and recurrent attacks of GA. Our findings thus suggest that NSAIDs not only inhibit nociception but also prevent the progression of osteolysis in chronic and repeated attacks of GA.

© 2020 THE AUTHORS. Published by Elsevier BV on behalf of Cairo University. This is an open access article under the CC BY-NC-ND license (<http://creativecommons.org/licenses/by-nc-nd/4.0/>).

Introduction

Deposition of monosodium urate (MSU) crystals which is a purine metabolite that is found in the synovial fluid of joints in most mammals is the major factor in Gouty arthritis (GA) [1,2]. In clinical practice, the normal diagnosis of GA is based on the concentration of uric acid in the serum or synovial fluid or of tophus material in the joints [1,3]. GA is also a kind of polyarthritis which is characterized by sudden onset and accompanied by severe pain in the joints of toes, fingers, ankles, shoulders, and knees [4]. Patients who do not receive effective urate-lowering therapy will progress to severe GA characterized by frequent arthritic flares and chronic inflammation that is often accompanied by pain and functional disability [5]. The deposition of MSU is the main cause of inflammation and joint swelling in GA. Accordingly, MSU crystals injection into the joints of animal models causes thermal hyperalgesia and mechanical allodynia [6–9]. MSU produces nociceptive stimulation that is accompanied by edematogenic responses in the joints that could be mediated by different infiltrating inflammatory cells, such as neutrophils, mast cells, and other leukocytes, as well as by inflammatory cytokines, including inducible nitric oxide synthase (iNOS), cyclooxygenase-2 (COX-2), and interleukin-1 β (IL-1 β), among others [3,7,10]. In terms of animal models of gout, most researchers have used air pouch models and MSU-induced models that can only be utilized to evaluate the acute phase of inflammatory change and cytokine release in acute gout attacks [7,11–13]. However, the frequent arthritic flares of GA that lead to chronic phase (including inflammation and pain) also play important roles in GA [4]. Thus, the progression of the chronic phase of GA still needs to be clarified through investigations of more suitable animal models.

MSU crystal deposition is also associated with the joint dysfunction seen in the chronic phase of clinical GA [14,15]. Advanced imaging modalities used in clinical diagnosis, including magnetic resonance imaging (MRI), ultrasonography and micro-computed tomography (micro-CT) imaging, have demonstrated that chronic tophaceous GA can cause osteolysis [15–19]. However, the majority of previous animal studies have focused on MSU-induced acute GA without making observations regarding osteolysis [11,20,21]. In our own previous study, osteoclastic-related proteins (cathepsin K and matrix metalloproteinase (MMP)-9) of the joints were observed in MSU-induced acute GA but without apparent cartilage damage and bone erosion [22]. In contrast, in clinical observation, frequent arthritic flares of severe and chronic tophaceous gout would enhance the osteoclastogenesis of erosive joint damage seen in long-term functional impairment [21,23]. Pineda et al. indicated that the injection of MSU in a rabbit model could change the joint structure in the early phase to mimic the characteristics of GA in humans [17]. Our own previous study found that acute GA was accompanied by the upregulation of the osteoclastic-related proteins TRAP, cathepsin K, and MMP-9 in the joint tissues of MSU-treated rats. However, the details of osteoclastogenesis or osteolysis process in this MSU-induced chronic and recurrent GA model were still unclear. Therefore, in the present study, we sought to establish chronic, recurrent, and frequent MSU-induced arthritic flares of GA accompanied by progressive osteolysis in rats.

It has long been known that frequent arthritic flares lead to osteolysis through osteoclastogenesis [15–19]. Osteoclasts are

differentiate from monocyte/macrophage lineage and are responsible for bone resorption [21]. The upregulation of osteoclasts in inflamed joints would lead to a broke balance between bone resorption and formation [24]. Cathepsin K and MMPs, which are expressed by osteoclasts, chondrocytes, and infiltrating cells, can cause collagen degradation and bone loss [15,24,25]. The activation of osteoclastogenesis primarily involves the receptor activator of nuclear factor γ -B (RANK) and the RANK ligand (RANKL) pathway, which is upstream for the expression of cathepsin K and MMPs [15,24]. McQueen et al. demonstrated that MSU-induced osteoclastogenesis results in joint destruction via promotion of the RANK/RANKL pathway and osteoclast maturation in GA [15]. Orally administered non-steroidal anti-inflammatory drugs (NSAIDs) and colchicine are the first-line agents for the systemic treatment of the acute phase of GA, and NSAIDs are a convenient and well-accepted option for treating GA in the absence of contraindications. However, while NSAIDs can improve the acute pain and inflammation of acute GA by reducing pro-inflammatory mediator production and the infiltration of inflammatory cells into the joint tissue [3,26]. The preventive effects of NSAIDs against chronic and recurrent GA-induced osteoclastogenesis still need to be examined in the chronic phase of GA.

In the present study, therefore, we evaluated the nociceptive behaviors and immunohistopathology of the joints of rats with chronic and recurrent attacks of GA induced by intra-articular injections of MSU (2 times/week for 10 weeks). Moreover, we also examined the effects of the NSAID, etoricoxib on the MSU-induced nociceptive behaviors and the progression of osteolysis in those rats. To evaluate the morphometric change of the joint structure, micro-CT analysis and histopathological analysis (safranin O/fast green staining) were performed to observe the joint destruction. Furthermore, immunohistochemical and TRAP stainings were performed to clarify the role of osteoclastogenesis in the process of osteolysis, as well as the beneficial effects of etoricoxib in chronic and repeated attacks of GA.

Materials and methods

Animals

In this study, we used wistar rats (250–300 g) for inducing chronic GA which got from LASCOS Inc., Taipei, Taiwan. Rat were kept in plastic cages with freely available fodder and water, and controlled temperature (24 ± 2 °C) with a 12-h light/dark cycle. The use of rats complied with the Guiding Principles in the Care and Use of Animals as approved by the Council of the American Physiology Society and approved by the institutional Animal Care and Use Committee of National Sun Yat-Sen University (approve number: 10424 and 10537). All experiments are made to minimize rats suffering and reduce the number of rats used.

Preparation of MSU and chronic, recurrent attacks of gouty arthritis model

The method of MSU crystals preparation was following the method reported by Seegmiller et al. [23]. Briefly, uric acid (catalog No. 1198772, Sigma, St. Louis, MO, USA) was dissolved in boiling water (1 g in 200 ml with 6 ml of 1 N NaOH). PH value was

adjusted to 7.2 by HCl. We have stirred and cooled the solution to room temperature, and stored at 4 °C overnight. The precipitate was filtered with filter paper and dried under low heat to obtain MSU crystal. The MSU crystals were mixed with phosphate-buffered saline (PBS, 2.5 mg/0.1 ml PBS) for injecting into the medial side of the knee (intra-articular (i.a.) knee injection) of each rat under 2.5% isoflurane. More specifically, to establish a chronic, recurrent attacks of GA model, we injected MSU into the knee of each rat two times per week from the 1st through 10th weeks.

Experimental design

Rats used were stochastically divided into 4 groups: control group (n = 6) received PBS injection into the knee two times per week from the 1st through 10th weeks. MSU group (n = 6) received MSU injections into the knee two times per week from the 1st through 10th weeks. MSU + etoricoxib group (n = 6) was orally administered etoricoxib (18 mg/kg) two times per week 6 h after each MSU injection in the knee from the 1st through 10th weeks. Etoricoxib alone group (n = 6) was only orally administered etoricoxib (18 mg/kg) two times per week from the 1st through 10th weeks. The nociceptive behaviors and joint swelling of the rats in each group were observed and measured from the 1st through 10th weeks. The rats were then sacrificed at the 10th week and subjected to micro-CT analysis, histopathological analysis, TRAP staining, and immunochemical staining.

Joint width measurement

To measure the knee joint width of rats. The vernier calipers (Aesculap, Germany) were used to measure the medial side to the lateral side of the knee at the level of the medial to the lateral joint lines.

Nociceptive behaviors

Mechanical allodynia

To measure the mechanical allodynia of rats, the calibrated von Frey filaments (North Coast Medical, Inc. Morgan Hill, CA, USA) was used. A series of von Frey filaments (the rage of stiffness is 0.2–15 g) were used to measure on the mid-plantar hind paw site. The chaplan's "up-down" method was followed by involved the use different fibers with used to determine the 50% withdrawal threshold with 5 s touch time and 5 times during 3-min intervals [27]. The positive response is mean that are any discomfort action (exp: vocalization, flinching) or attempt to withdraw the paw [8,27].

Thermal hyperalgesia

To measure the thermal hyperalgesia of rats, the IITC analgesimeter (IITC Inc., Woodland Hills, CA, USA) were used and was following from previous studies [28–30]. Briefly, we placed the rats into brown plastic box on top of an elevated glass plate. The heat stimulator was positioned and directed onto the mid-plantar site of hind paw with using a low-intensity heat (active intensity = 25). Record the respond time of a positive response (licking or withdrawal). Paw withdrawal latency (seconds) was record with a cut-off time (30 s) and use the average of more than 2 time per paw response [28,30].

Weight-bearing distribution

To measure the distribution of weight-bearing on the hind paw, the channel weight averager (Sigma Technology Corporation, TW) which independently measured each hind paw was used. The dif-

ference of weight-bearing on hind paw was adopted as index for joint discomfort and was determined. Briefly, rats were placed into brown plastic chamber and checked each hind paw rested on a separated force plate. For assess the weight bearing of each hind paw (in grams), the average of 5-s period was detected and each data point is the mean of 3 during 5-s readings. The difference between right (ipsilateral) and left (contralateral) expressed as the hind paw weight distribution [31].

Sample preparation of knee

At 10th weeks, we sacrificed the rats by deep anesthesia with 2.5% isoflurane and perfused intracardially with 0.4 L PBS (contain 1% sodium nitrite and 0.2 U/mL heparin). And the rats were perfused intracardially by 4% paraformaldehyde in PBS. We collect the knee of the hind limb and fixed that samples in 10% neutral formalin for one week at 4 °C for micro-CT scanning. And then knee samples were then decalcified for histopathological evaluation and immunohistochemical staining.

Micro CT imaging

Three-dimensional reconstructions of the rat knees were obtained by micro focal computed tomography (Skyscan 1076, Bruker, MA, USA) performed by the Taiwan Mouse Clinic, Taiwan. For each rat, the proximal ends of the right tibia were scanned with a voxel size of 9 µm. The x-ray tube voltage was 50 kV, and the current was 140 µA, with a 0.5 mm aluminum filter. Each scan was carried out through 180 degrees, with a rotation step of 0.8 degrees and an exposure time of 3300 ms at each step. For analysis of the subchondral plate, the region of interest with an area of $1.6 \times 1.5 \text{ mm}^2$ was selected. Bone mineral density and the thickness of the subchondral plate were measured and calculated. For analysis of the subchondral trabecular bone, a cuboid of trabecular bone with a size of $1.6 \times 1.5 \times 0.6 \text{ mm}^3$ beneath the region of interest (ROI) of the subchondral plate was selected. The trabecular thickness, trabecular separation, and trabecular number were calculated for the subchondral trabecular bone.

Histopathological evaluation

12.5% ethylenediaminetetraacetic acid (EDTA) in PBS (2–3 weeks) was used for sample decalcification (2–3 weeks). We deparaffinized and dehydrated the samples by xylene and ethanol (Tissue-Tek, Sakura Finetek Japan Co., Ltd, Japan) and embedded in paraffin. 2-µm sections (HM340E, Microm, Biotechnical Services, Inc., USA) were prepared for histopathological evaluation. These staining sections were analyzed under by microscope (DM 6000B, Leica Inc., Germany) with image output system (idea SPOT, Diagnostic instruments Inc., USA). The method of histopathological evaluation is modify from Gerwin et al. and Kao et al. for cartilage degeneration score, total cartilage degeneration width, significant cartilage degeneration width and zonal depth ratio of lesions with safranin-O/fast green staining images [32,33].

Tartrate-resistant acid phosphatase (TRAP) staining

To measure osteoclast markers, the section was staining by TRAP staining (Sigma-aldrich, catalogue no. 386A, Saint Louis, MO, USA) with according to the instructions of the manufacturer. Briefly, we deparaffinized and dehydrated the samples by xylene and alcohol. Samples were covered with fixative buffer for 30 s and then rinsed in deionized water. Naphthol AS-BI phosphoric acid solution and Fast Garnet GBC base solution (Sigma-aldrich, catalogue no. 386A, Saint Louis, MO, USA) were used for TRAP staining with cover samples for 2 h at 37 °C. The samples were then

washed with pure water and counterstained with hematoxylin. Each section was observed and recorded by upright microscope with image capture system. The calculating average of TRAP-positive cells was analyzed under 200 \times magnification in six different fields.

Immunohistochemistry

The method of immunohistochemical staining for rat knee sample as follow the previous studies [22,29,31]. Briefly, the sections were deparaffinized and dehydrated by xylene and ethanol. Endogenous peroxidase was quenched by H₂O₂ (3%), and the antigen were retrieved by proteinase K (20 mM; Sigma, St Louis, MO, USA). The 4% normal horse serum in PBS was used for minimizing the non-specific adsorption. And the sections were incubated with primary anti-bodies, including anti-cathepsin K (1:100; Abcam; catalogue no. ab25916; polyclonal antibody), anti-MMP9 (1:100; Abcam; catalogue no. ab76003; monoclonal antibody) and anti-MMP13 (1:100; Abcam; catalogue no. ab39012; polyclonal antibody) at overnight at 4 °C, respectively. Biotin-conjugated anti-rabbit IgG (Vector Laboratories, Burlingame, CA, USA) and avidin-biotin peroxidase in combination with an ABC kit (Vectastain ABC kit; Vector Labs, Burlingame, CA, USA) were used for specific labeling. And we use 3,3'-diaminobenzidine tetrahydrochloride (DAB) to react with sample. Each section was analyzed by microscope and image output system. We acquired the immunoreactive positive cell on 200 \times magnification in six fields.

Double-immunofluorescent staining

For double-immunofluorescent staining of RANKL with osteoblast markers (osteocalcin) [34], the paraffin sections were incubated with a mixture of anti-RANKL (1:200 dilution, cat. Sc-7628; Santa Cruz; polyclonal goat antibody) with anti-osteocalcin (1:200 dilution cat. Orb1266; polyclonal rabbit antibody) antibodies. And the second antibody was the mixture of Alexa Fluor 488-conjugated chicken anti-mouse IgG antibody (1:200 dilution; cat. A-21200; Molecular Probes, Eugene, OR, USA; green fluorescence) and DyLight 549-conjugated donkey anti-rabbit IgG antibody (1:400 dilution, cat. 711-506-152; Jackson ImmunoResearch Laboratories Inc., West Grove, PA, USA; red fluorescence) was used for incubated with the section for 90 min at room temperature. The confocal images were acquired using a Leica TCS SP5 II confocal microscope (Leica Instruments, Wetzlar, Germany).

Statistical analysis

All data are presented as mean \pm SEM. The data for nociceptive behaviors; knee swelling; micro CT analysis; and the quantitation of TRAP-, cathepsin K-, MMP-9-, and MMP-13-positive cells were analyzed by Kruskal–Wallis one-way analysis of variance after normality test. And one-way analysis of variance followed by the Student–Newman–Keuls post hoc test was used for analyzed other data. *P* values less than 0.05 were considered significant difference.

Result

Effects of etoricoxib on inflammatory response of MSU-induced chronic, recurrent attacks of GA model.

Fig. 1A shows the effects of recurrent injections of MSU into a knee joint in terms of the differences between bilateral knee joints. The results showed that recurrent injections of MSU could progressively increase the mean joint size from 0.57 ± 0.18 mm

to 3.41 ± 0.18 mm by the 10th week. Furthermore, the oral administration of etoricoxib after MSU injection resulted in the width of the knee joint being increased from 0.04 ± 0.05 mm to 2.5 ± 0.1 mm by the 10th week. Meanwhile, the oral administration of etoricoxib without MSU injection did not result in any change in swelling of the knee compared to the control group. Representative macroscopic photographs of the recurrent MSU injections into the knee joint are shown in Fig. 1B. The MSU group presented swelling of the knee after the recurrent injections of MSU into the knee joint. However, the oral administration of etoricoxib could effectively reduce the swelling after MSU injections into the knee joints of rats.

Effects of etoricoxib on recurrent MSU injection induced nociceptive behaviors

Fig. 1C shows, however, that the effects of the recurrent injections of MSU into the knee joint induced thermal hyperalgesia. The mean paw withdrawal latency of the MSU group progressively decreased from 20.6 ± 2.2 s to 13.5 ± 1.9 s in the 10th week. Meanwhile, the oral administration of etoricoxib after MSU injection resulted in the paw withdrawal latency being decreased from 27.3 ± 0.8 s to 25.4 ± 0.5 s. These results showed that recurrent injections of MSU could aggravate thermal hyperalgesia but also that oral the administration of etoricoxib could significantly reduce the thermal hyperalgesia induced by the recurrent injections of MSU in rats. Fig. 1D and Fig. 1E show, respectively, that the recurrent injections of MSU progressively decreased the mean paw withdrawal threshold from 6.6 ± 0.2 g to 1.8 ± 0.8 g and increased the mean changes in hind paw weight distribution from 42.2 ± 2.6 g to 56.9 ± 7 g at the 10th week. Meanwhile, the oral administration of etoricoxib after MSU injection resulted in the paw withdrawal threshold being decreased from 6.8 ± 0.1 s to 6 ± 0.3 s at the 10th week and the changes in hind paw weight distribution being increased from 12.3 ± 6.1 g to 18 ± 9 g at the 10th week. In addition, the oral administration of etoricoxib without MSU injection did not result in any significant differences in nociceptive behaviors compared to the control group. The above results indicated that the administration of etoricoxib could attenuate the thermal hyperalgesia, mechanical allodynia, and weight bearing distribution effects of MSU-induced chronic, recurrent attacks of GA in rats.

Micro CT analysis of etoricoxib on MSU-induced chronic, recurrent attacks of GA

Fig. 2A illustrates that the bone contact was high and the surfaces of the knee joints were smooth in control rats. In addition, there was no bone erosion on the subchondral plate visible in the sagittal views of the control group. In contrast, obvious bone destruction of the surface of the knee joints was observed in the MSU group. Furthermore, there was clear bone erosion on the subchondral plate visible in the sagittal views of the MSU groups. In comparison with the control group, there was also significantly lower bone mineral density (BMD) (0.48 ± 0.008 gcm⁻³ for the control group and 0.41 ± 0.016 gcm⁻³ for the MSU group, *p* = 0.05) and subchondral plate thickness (0.23 ± 0.006 mm of control group and 0.16 ± 0.003 mm for MSU group, *p* \leq 0.001) in the MSU group (Fig. 2B & C). Meanwhile, etoricoxib markedly attenuated the MSU-induced joint destruction on the surfaces of the knee and the bone erosion of the subchondral plate. In comparison with the MSU group, there was significantly higher BMD (0.41 ± 0.016 gcm⁻³ for MSU group and 0.46 ± 0.009 gcm⁻³ for MSU + etoricoxib group, *p* = 0.026) and subchondral plate thickness (0.16 ± 0.003 gcm⁻³ for MSU group and 0.21 ± 0.004 gcm⁻³ for MSU + etoricoxib group, *p* \leq 0.001) in the MSU + etoricoxib group (Fig. 2B & C). Also,

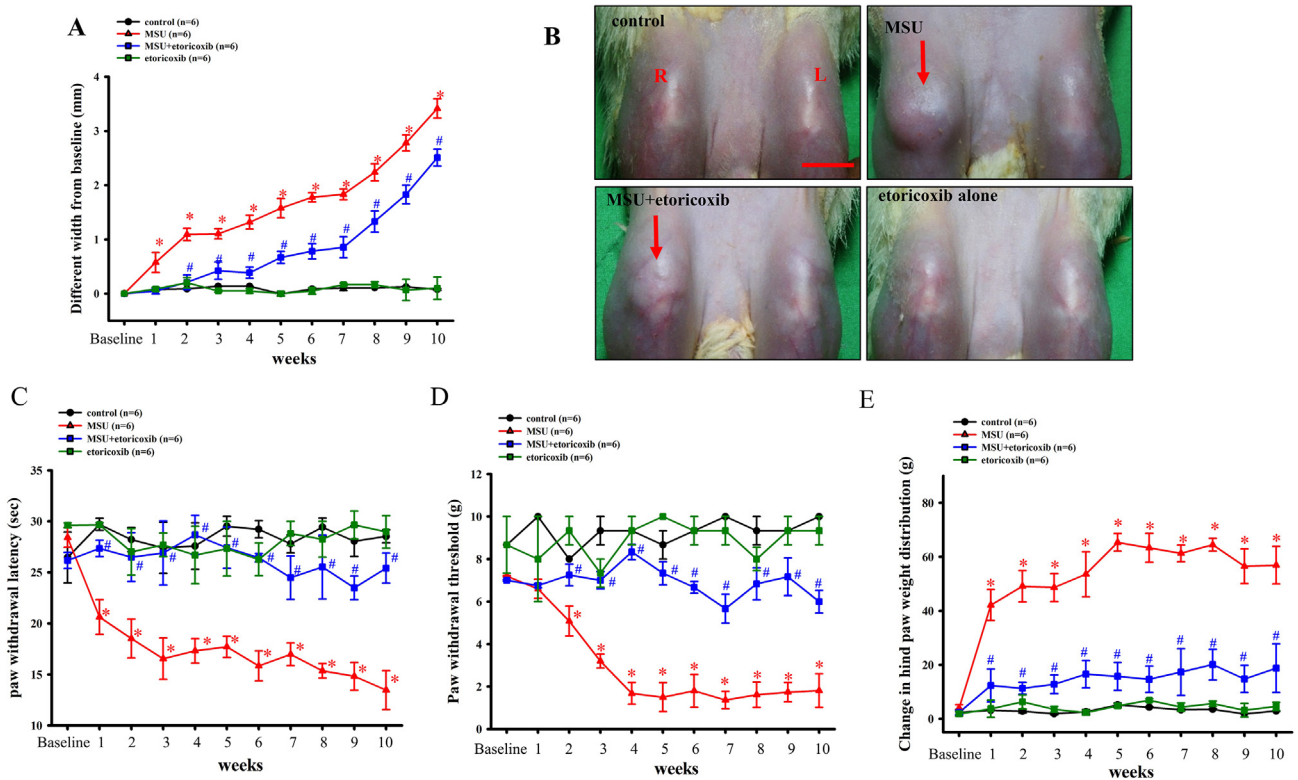


Fig. 1. MSU to induce chronic and recurrent attacks of GA model. Time courses of the effects of etoricoxib on MSU-induced knee swelling (A), thermal hyperalgesia (C), mechanical allodynia (D), and hind paw weight-bearing deficits (E) in chronic GA. Oral administration of etoricoxib reduced MSU-induced knee swelling in the GA model. Each value show as mean \pm SEM for each group. Results demonstrate that MSU significantly induced nociceptive behaviors and knee swelling and that etoricoxib could significantly reduce those effects. (B) Representative macroscopic images of the knee from the control, MSU, MSU + etoricoxib, and etoricoxib alone groups. Scale bar = 1 cm. * $p < 0.05$ symbolize significant variation between MSU and control groups at each time point. # $p < 0.05$ symbolize significant variation between MSU + etoricoxib and MSU group at each time point.

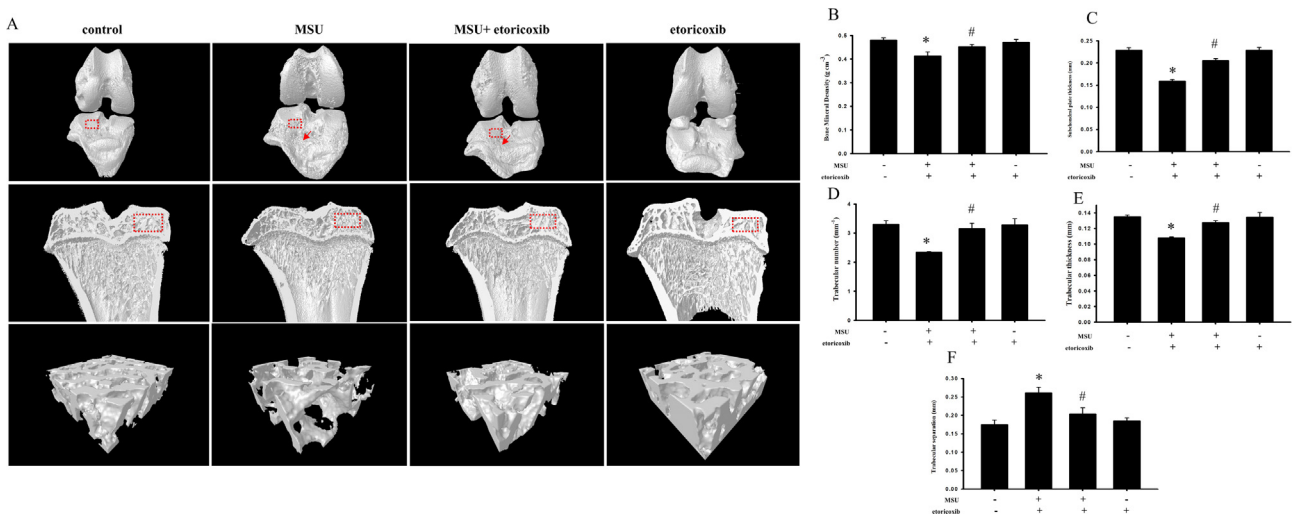


Fig. 2. Micro-CT scan on knee of MUS-induced chronic, recurrent attacks of GA model. (A) Representative three-dimensional renderings of surface of knee, sagittal views, and trabecular bone scanned by micro-computed tomography. Red arrow indicates apparent bone erosion on surface of knee. Quantitative analysis of BMD (B), subchondral plate thickness (C), trabecular number (D), trabecular separation (E), and trabecular thickness (F), and analysis ROI (red frame) from surface of knee and sagittal views, respectively. * $p < 0.05$ symbolize significant variation between MSU and control groups. # $p < 0.05$ symbolize significant variation between MSU + etoricoxib and MSU group. (For interpretation of the references to color in this figure legend, the reader is referred to the web version of this article.)

there was no significant structure change of the subchondral plate in etoricoxib alone group compared to the control group. The subchondral trabecular bone was also examined and analyzed by micro-CT. The region of interest (red box) of the subchondral trabecular bone is shown in the sagittal views of each group. In

comparison with the control group, there were significant decreases of trabecular bone number ($3.3 \pm 0.12 \text{ mm}^{-1}$ for control group and $2.3 \pm 0.02 \text{ mm}^{-1}$ for MSU group, $p \leq 0.001$) and trabecular bone thickness ($0.14 \pm 0.002 \text{ mm}$ of control group and $0.11 \pm 0.001 \text{ mm}$ for MSU group, $p \leq 0.001$) and a significant

increase of trabecular separation (0.17 ± 0.012 mm of control group and 0.26 ± 0.015 mm for MSU group, $p = 0.00$) in the MSU group (Fig. 2D-F). In comparison with the MSU group, meanwhile, the trabecular bone number (2.3 ± 0.02 mm⁻¹ for MSU group and 3.15 ± 0.19 mm⁻¹ for MSU + etoricoxib group, $p = 0.002$) and trabecular bone thickness (0.11 ± 0.001 mm of MSU group and 0.13 ± 0.002 mm for MSU + etoricoxib group, $p \leq 0.001$) were significantly higher and the trabecular separation (0.26 ± 0.015 mm of MSU group and 0.2 ± 0.04 mm for MSU + etoricoxib group, $p = 0.025$) was significantly lower in the MSU + etoricoxib group. At the same time, there were no significant structure changes of the trabecular bone in the etoricoxib alone group compared to the control group.

Histopathological evaluation of etoricoxib on MSU-induced chronic, recurrent attacks of GA

To evaluate MSU-induced chronic, recurrent attacks of GA in rats, we prepared sections of knee joints from control, MSU, MSU + etoricoxib, and etoricoxib alone groups, and staining them with H&E stain for the synovial tissue and with safranin O/fast green for the cartilage and bone (Fig. 3). The images revealed the severe inflammation on synovial tissue, including the infiltration of numerous immune cells, in the synovial tissue of the MSU group, as well as the slight inflammatory response, including the infiltration of fewer immune cells, in the synovial tissue of the MSU + etoricoxib group. The safranin O/fast green staining revealed apparent cartilage and bone erosion in the MSU-rats, while also showing that the administration of etoricoxib reduced the cartilage and bone erosion in the MSU + etoricoxib group. Table 1 Fig. 3 presents a representative histopathological analysis of the cartilage degeneration score, total cartilage degeneration width, significant carti-

lage degeneration width, and zonal depth ratio of lesions. In comparison with the control group, there were significant increases in the cartilage degeneration score (0 ± 0 for control group and 13.5 ± 0.72 for MSU group, $p \leq 0.001$), total cartilage degeneration width, and significant cartilage degeneration width (0 ± 0 mm for control group and 10.7 ± 0.81 mm for MSU group, $p \leq 0.001$) of the MSU group. In comparison with the MSU group, meanwhile, the cartilage degeneration score (0 ± 0 mm for control group and 9.4 ± 1.10 mm for MSU group, $p \leq 0.001$), total cartilage degeneration width (10.7 ± 0.81 mm of MSU group and 2.1 ± 1.34 mm for MSU + etoricoxib group, $p \leq 0.001$), and significant cartilage degeneration width (9.4 ± 1.10 mm of MSU group and 0.5 ± 0.49 mm for MSU + etoricoxib group, $p = 0.025$) were significantly lower in the MSU + etoricoxib group (Table 1). Furthermore, there were no significant histopathological changes in etoricoxib alone group compared to the control group. Overall, the results indicated that the administration of etoricoxib could effectively lessen the histopathological changes resulting from recurrent MSU injections.

Effects of etoricoxib on TRAP positive cell of subchondral bone

The TRAP staining was used for the analysis of osteoclast formation, which plays an important role in joint destruction. Fig. 3A illustrates the distribution of TRAP-positive cells in the subchondral bone of knee joints from control, MSU, MSU + etoricoxib, and etoricoxib alone groups. The TRAP-positive cells appeared to be increased in the subchondral bone of the MSU group. In comparison with the control group, the number of TRAP-positive cell was significantly increased in the MSU group (0 ± 0 cells/mm² of control group and 46 ± 10 cells/mm² for MSU group, $p \leq 0.001$), whereas the administration of etoricoxib in the MSU + etoricoxib group reduced the MSU-induced increase in the number of TRAP-

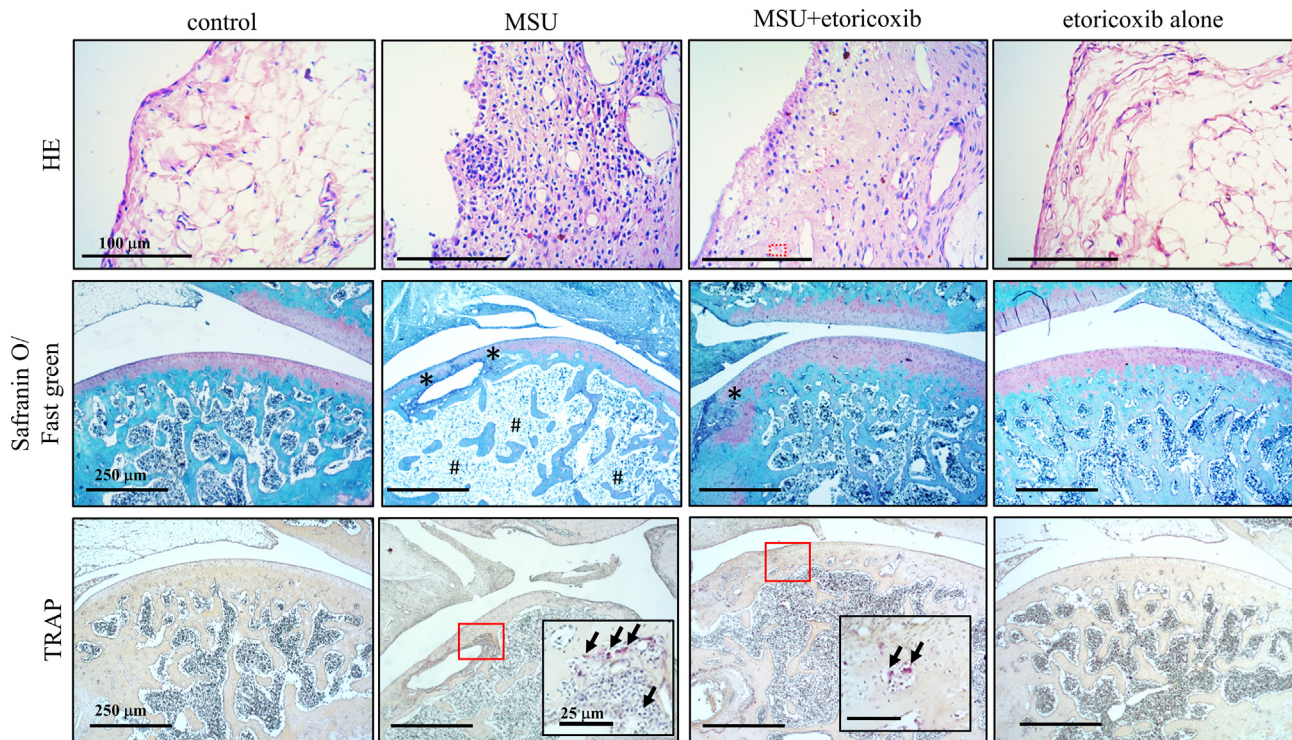


Fig. 3. Histopathological evaluation of MUS-induced chronic, recurrent attacks of GA model. Representative hematoxylin/eosin staining images for synovial tissue, Safranin O/Fast green staining images for cartilage and bone, and TRAP staining images for osteoclast of the knee joint sections of the control, MSU, MSU + etoricoxib, and etoricoxib alone groups. Oral administration of etoricoxib reduced that MSU-induced inflammation, cartilage damage, and osteoclast formation in the chronic GA model. * indicates apparent cartilage and bone erosion. Arrows indicate TRAP-positive cell. (For interpretation of the references to color in this figure legend, the reader is referred to the web version of this article.)

Table 1

Histopathological analysis. The representative histopathological analysis results of cartilage degeneration score, total cartilage degeneration width, significant cartilage degeneration width, zonal depth ratio of lesions, and quantitative analysis of TRAP-positive cells. * $p < 0.05$ symbolize significant difference between MSU and the control groups. # $p < 0.05$ symbolize significant difference between MSU + etoricoxib and the MSU group.

| | Control | MSU | MSU + etoricoxib | Etoricoxib alone |
|---|---------|--------------|------------------|------------------|
| Cartilage degeneration score | 0 ± 0 | 13.5 ± 0.72* | 1.3 ± 0.9# | 0 ± 0 |
| Total cartilage degeneration width (mm) | 0 ± 0 | 10.7 ± 0.81* | 2.1 ± 1.34# | 0 ± 0 |
| significant cartilage degeneration width (mm) | 0 ± 0 | 9.4 ± 1.10* | 0.5 ± 0.49# | 0 ± 0 |
| Zonal depth ratio of lesions | 0 ± 0 | 2.6 ± 0.17* | 0.7 ± 0.9# | 0 ± 0 |
| The number of TRAP positive cells (mm ⁻²) | 0 ± 0 | 46 ± 8.7* | 23.5 ± 5# | 0 ± 0 |

positive cell (46 ± 10 cells/mm² of MSU group and 23 ± 0.7 cells/mm² for MSU + etoricoxib group, $p = 0.049$). Meanwhile, there was no significant difference in the number of TRAP-positive cells between the control group and the etoricoxib alone group. Thus, taken together, the results indicated that recurrent MSU injections significantly promote osteoclast formation but that this promotion is inhibited by the administration of etoricoxib

Effects of etoricoxib on MMP-9, MMP-13 and cathepsin K protein expression of synovial tissue

Fig. 4A illustrates the distribution of MMP-9-, MMP-13-, and cathepsin K-positive cells in the synovial tissue of knee joints from the control, MSU, MSU + etoricoxib, and etoricoxib alone groups. The MMP-9-, MMP-13-, and cathepsin K-positive cells appeared

to be increased in the synovial tissue of the MSU group. In comparison with the control group, the numbers of MMP-9 (2.1 ± 1.48 cells/mm² of control group and 1991.4 ± 113.7 cells/mm² for MSU group, $p \leq 0.001$), MMP-13 (3.6 ± 2.53 cells/mm² of control group and 1361.0 ± 42.60 cells/mm² for MSU group, $p \leq 0.001$), and cathepsin K (7.1 ± 2.78 cells/mm² of control group and 1194.6 ± 73.12 cells/mm² for MSU group, $p \leq 0.001$) positive cells were significantly up-regulated in the MSU group (Fig. 4B-D). However, the administration of etoricoxib in the MSU + etoricoxib group reduced this MSU-induced increase in the numbers of MMP-9 (1991.4 ± 113.7 cells/mm² of MSU group and 1042.4 ± 27.91 cells/mm² for MSU + etoricoxib group, $p \leq 0.001$), MMP-13 (1361.0 ± 42.60 cells/mm² of MSU group and 823.5 ± 57.99 cells/mm² for MSU + etoricoxib group, $p \leq 0.001$), and cathepsin K (1194.6 ± 73.12 cells/mm² of MSU group and 799.8 ± 54.10

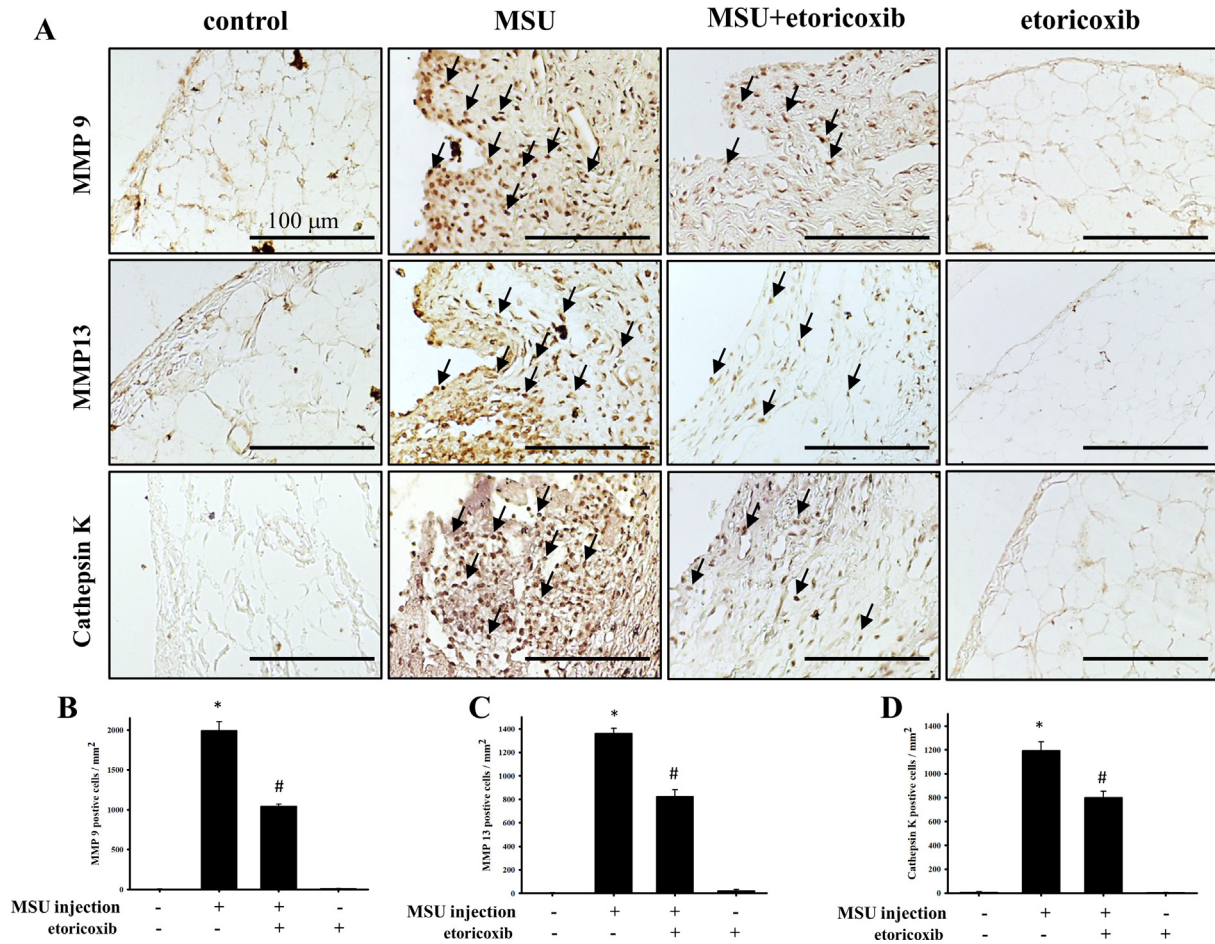


Fig. 4. Immunohistochemical staining of MMP-9, MMP-13, and cathepsin K in synovial tissue. (A) Positive cells are indicated in brown (arrows) in joint sections from the control, MSU, MSU + etoricoxib, and etoricoxib alone groups. Quantitative analysis results of MMP-9- (B), MMP-13- (C), and cathepsin K- (D) positive cells of the synovial tissue are shown. Each value show as mean ± SEM for each group. Scale bar = 100 μm. * $p < 0.05$ symbolize significant variation between MSU and the control groups. # $p < 0.05$ symbolize significant variation between MSU + etoricoxib and MSU group.

cells/mm² for MSU + etoricoxib group, $p = 0.001$) positive cells. Meanwhile, no significant differences in the numbers of MMP-9-, MMP-13-, and cathepsin K-positive cells in synovial tissue between the control and etoricoxib alone group be observed. Thus, taken together, the results indicated that recurrent MSU injections significantly up-regulate MMP-9, MMP-13, and cathepsin K in synovial tissue but that this up-regulation is inhibited by the administration of etoricoxib.

Effect of etoricoxib MMP-9 MMP-13 and cathepsin K protein expression of cartilage

Fig. 5A illustrates the distribution of MMP-9-, MMP-13-, and cathepsin K-positive cells in the cartilage of knee joints from the control, MSU, MSU + etoricoxib, and etoricoxib alone groups. The MMP-9-, MMP-13-, and cathepsin K-positive cells appeared to be increased in the cartilage of the MSU group. In comparison with the control group, the numbers of MMP-9 (0 ± 0 cells/mm² of control group and 784.9 ± 52.12 cells/mm² for MSU group, $p \leq 0.001$), MMP-13 (0 ± 0 cells/mm² of control group and 913.7 ± 109.71 cells/mm² for MSU group, $p \leq 0.001$), and cathepsin K (42.0 ± 12.02 cells/mm² of control group and 409.3 ± 11.02 cells/mm² for MSU group, $p \leq 0.001$) positive cells were significantly up-regulated in the MSU group, while the administration of etoricoxib in the MSU + etoricoxib group reduced this MSU-induced increase

in the numbers of MMP-9 (784.9 ± 52.12 cells/mm² of MSU group and 621.2 ± 24.60 cells/mm² for MSU + etoricoxib group, $p = 0.004$), MMP-13 (913.7 ± 109.7 cells/mm² of MSU group and 598.9 ± 55.99 cells/mm² for MSU + etoricoxib group, $p = 0.007$), and cathepsin K (409.3 ± 11.02 cells/mm² of MSU group and 150.6 ± 35.01 cells/mm² for MSU + etoricoxib group, $p \leq 0.001$) positive cells (Fig. 5B-D). Meanwhile, no significant differences in the numbers of MMP-9-, MMP-13-, and cathepsin K-positive cells in cartilage between control and etoricoxib alone group be observed. Thus, taken together, the results indicated that recurrent MSU injections significantly up-regulate MMP-9, MMP-13, and cathepsin K protein expressions in cartilage but that this up-regulation is inhibited by the administration of etoricoxib.

Effect of etoricoxib on RANKL and osteocalcin on bone marrow of subchondral bone marrow

To further confirm the participation of the RANK/RANKL pathway in the recurrent and chronic MSU-induced joint destruction of GA, we also used confocal microscopy to observe RANKL-positive cells with osteocalcin (a marker of osteoblasts) in subchondral bone marrow. Fig. 6 demonstrates that the RANKL-positive cells (Green color) were apparent in the MSU group, while the administration of etoricoxib in the MSU + etoricoxib group could reduce the number of RANKL-positive cells. Similar effects

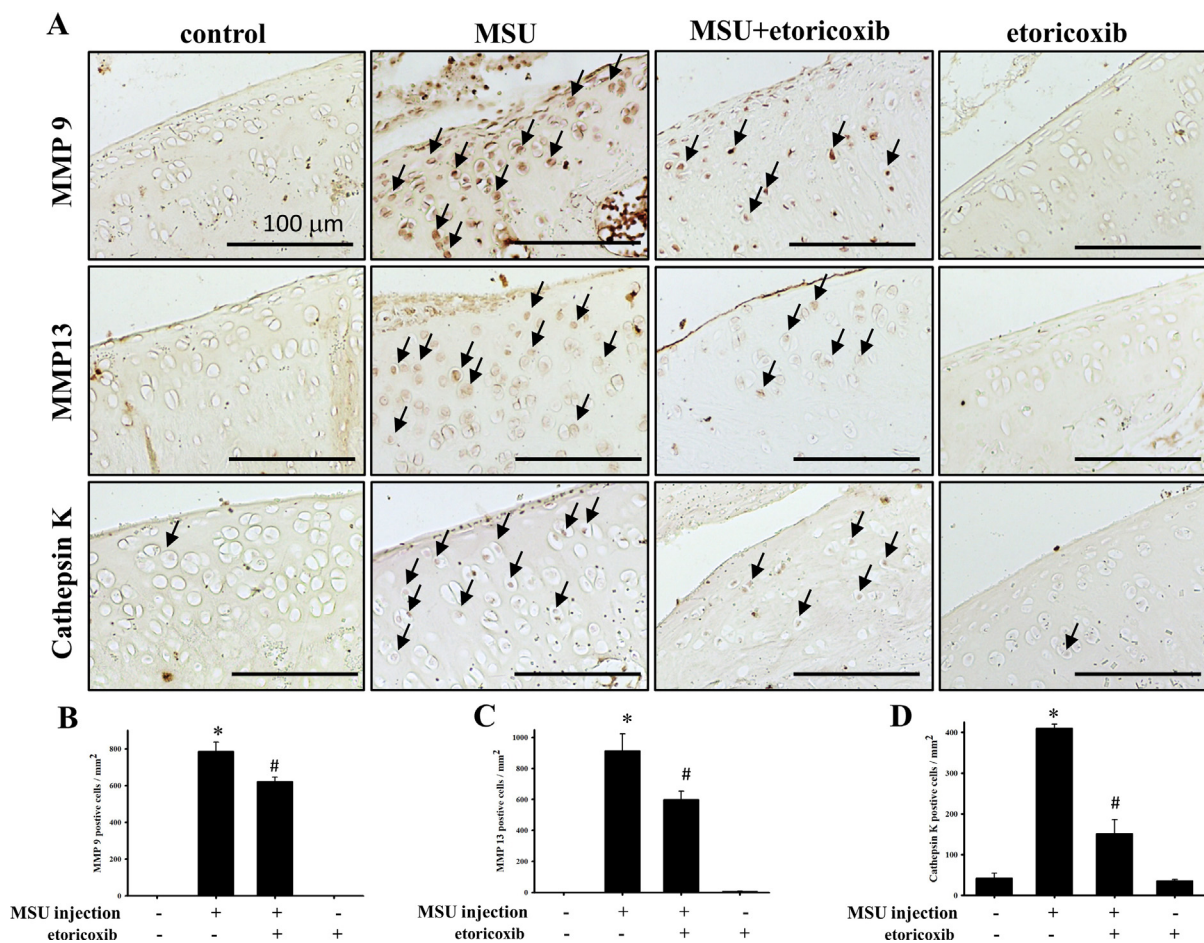


Fig. 5. Immunohistochemical stain of MMP9 MMP13 and cathepsin K on cartilage of knee. (A) Positive cells is shown in red-brown (arrow) in ankle joint sections from control, MSU, MSU + etoricoxib groups and etoricoxib alone groups. (B) Quantitative analysis of MMP 9 (B), MMP 13 (C) and cathepsin K (D) positive cell on cartilage are shown. Each value show as mean \pm SEM for each group. Scale bar = 100 μ m. * $p < 0.05$ symbolize significant variation between MSU and the control groups. # $p < 0.05$ symbolize significant variation between MSU + etoricoxib and the MSU group. (For interpretation of the references to color in this figure legend, the reader is referred to the web version of this article.)

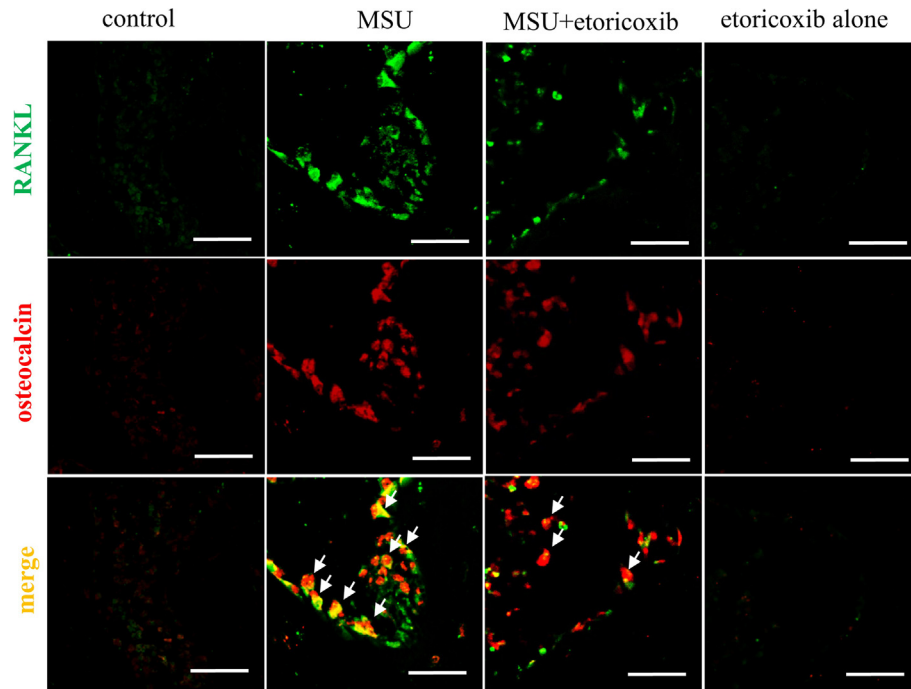


Fig. 6. Immunofluorescence staining of RANKL and osteocalcin in bone marrow of subchondral bone marrow. Representative confocal microscopy images showing the localization of RANKL (green) and osteocalcin (red) in subchondral bone marrow of the control, MSU, MSU + etoricoxib, and etoricoxib alone groups. Colocalization is symbolize by yellow color and arrows. The results showed that RANKL is primarily colocalized with osteoblasts. Scale bars = 50 μm . (For interpretation of the references to color in this figure legend, the reader is referred to the web version of this article.)

on osteocalcin-positive cells were observed in the MSU and MSU + etoricoxib groups. In addition, localization with RANKL- (Green color) and osteocalcin- (red color) positive cells in the subchondral bone marrow of control, MSU, MSU + etoricoxib, and etoricoxib alone groups was demonstrated by double-labeling immunofluorescent staining. Merged images shown that RANKL colocalized with osteocalcin (yellow, white arrow). Thus, osteoblasts in the subchondral bone marrow of the MSU rats were the major cell type expressing RANKL in GA, while the administration of etoricoxib reduced the secretions of osteoblasts and the expression of RANKL in GA. Meanwhile, there were no apparent RANKL- or osteocalcin-positive cells in the etoricoxib alone group. Thus, the results indicated that the administration of etoricoxib attenuates recurrent MSU injection-induced osteoblast expression of RANKL in GA.

Discussion

In this study, we investigated chronic and recurrent attacks of GA induced by recurrent intra-articular injections of MSU in rats. In doing so, we examined the nociceptive behaviors and chronic inflammatory responses in the chronic and recurrent phase of GA. Our results showed that the oral administration of etoricoxib could effectively inhibit the chronic nociceptive behaviors and reduced joint edema of chronic GA. Specifically, we demonstrated osteolysis in an MSU-induced chronic and recurrent GA rat model. The micro-CT analysis and histopathological evaluation results showed that significant osteolysis and inflammation were induced by recurrent injections of MSU. In addition, evaluations of osteoclastogenesis and related protein (cathepsin k, MMP 9 and MMP13) were performed by TRAP staining and immunohistochemical staining. The double-immunofluorescent staining results illustrated that RANKL-positive osteoblasts were upregulated by the recurrent MSU injections and that osteoclastogenesis was promoted in chronic GA.

In clinical practice, GA is considered a form of chronic pain and inflammatory arthritis. According to epidemiological statistics, it affects about 1–4% of the general population (about 5% of men and 1% of women), and up to 80% of patients will experience a recurrent attack within 3 years [1,3]. Moreover, diagnosis is usually made clinically, supported by the presence of hyperuricemia, which would induce the deposition of MSU under normal conditions [1,2]. GA patients suffering from burning sensations and/or allodynia have been reported, and the thermal hyperalgesia and mechanical allodynia in acute gout animal models have previously been measured [7,35,36]. Frequent stimulation with MSU would lead to chronic inflammation and pain with edematogenic responses in the joints that could be accompanied by increased levels of different infiltrating inflammatory cells and inflammatory mediators [3,7,10]. Several previous studies, including our own, have demonstrated that leukocyte infiltration and pro-inflammatory proteins, such as iNOS, COX-2, and c-fos, play important roles in MSU-induced acute gout animal models [8,37,38]. In this study, our results demonstrated that the time-course effects of recurrent MSU injections include the significant aggravation of nociceptive behaviors accompanied by increasing swelling of the joint. Typical representative macroscopic photographs and histopathological evaluations showed obvious inflammatory responses after recurrent injections of MSU. Furthermore, immunohistochemical analysis showed that MMP-9-, MMP-13-, and cathepsin K-positive cells, which also play significant roles in inflammatory responses, were upregulated in synovial tissues [39,40]. Orally administered NSAIDs and colchicine are the first-line agents for systemic treatment of the acute phase of GA in clinical practice, and NSAIDs are a convenient and well-accepted option for treating GA in the absence of contraindications [3,26]. Relatedly, while the anti-inflammatory property of colchicine has been explained, NSAIDs have been shown to be a better option for the analgesic treatment of GA in clinical contexts [41]. Moreover, the higher toxicity (1.2 mg/daily in humans) and lower toler-

ability (2 mg/daily in humans) of colchicine have been found to be harmful to patients, including the induction of adverse gastrointestinal effects [42]. In one study, NSAIDs were found to have better tolerability and lower toxicity than colchicine in humans. Thus, etoricoxib (60–120 mg/daily for human), which is also a drug used clinically to treat GA, was used as a positive control in this experiment [43]. The results showed that the administration of etoricoxib could inhibit the chronic nociception and decrease the joint swelling resulting from frequent stimulation with MSU. Typical representative macroscopic photographs and histopathological evaluations also illustrated that such inflammatory responses could be ameliorated by etoricoxib treatment. Moreover, MMP-9, MMP-13-, and cathepsin K-positive cells were also downregulated after the oral administration of etoricoxib and frequent stimulation with MSU. Therefore, our data suggested, among other things, that frequent stimulation with MSU could induce and aggravate chronic nociceptive behaviors and inflammation in rats in a manner approximating the chronic and severe phase of GA in humans.

Joint damage is a late feature of GA and includes cartilage damage and bone erosion, which have been shown to be closely associated with MSU crystal deposition inducing inflammatory responses [37]. In previous histological studies, MSU crystals were found to be frequently deposited within or adjacent to cartilage and to lead to cartilage damage and bone erosion in patients [37,44]. Accurate imaging modalities, namely, micro-CT and MRI, have revealed the abnormalities in joints seen in clinical practice are caused by MSU crystal deposition [15,45]. Relatedly, CT is probably a more accurate imaging tool for the definition of MSU crystals-induced bone erosion. Pineda et al. indicated that the injection of MSU in a rabbit model could change the joint structure in the early phase to mimic the characteristics of GA in humans. In this study, the micro-CT images revealed bone erosion on the surfaces of knees with decreases in subchondral plate thickness after recurrent injections of MSU. In past clinical research, the changes in subchondral structures induced by tophi deposition have been described via MRI, CT, and ultrasonography [45,46]. The bone marrow edema of severe GA can also be detected through MRI or CT [46,47]. In the present study, the trabecular bone was scanned by micro-CT, and significant decreases of BMD, trabecular number, and trabecular thickness, as well as a significant increase in trabecular separation, were detected. Moreover, the histological results indicated that the cartilage degeneration score and width, as well as the zonal depth ratio of lesions, of the MSU group showed significant differences compared to the control group. In addition, immunohistochemical staining demonstrated that recurrent injections of MSU upregulated MMP-9, MMP-13, and cathepsin K protein expression in chondrocytes. Thus, recurrent injections of MSU promote joint destruction. However, the oral administration of etoricoxib could significantly improve the cartilage and bone erosion in this MSU-induced chronic, recurrent GA model. Therefore, recurrent injections of MSU imitate the clinical characteristics of the severe phase of GA, while the administration of etoricoxib not only attenuates nociceptive behaviors but also improves the joint damage caused by chronic GA.

In our previous study, osteoclast-related proteins (including cathepsin K and MMP-9) in the joint were observed in MSU-induced acute gout but without apparent cartilage damage and bone erosion [22]. In the present study, our micro-CT analysis revealed that significant osteolysis could be induced by recurrent injections of MSU. The histopathological evaluations further demonstrated cartilage damage and synovial inflammation, while the upregulation of the number of TRAP-positive cells indicated that osteoclastogenesis could play an important role in the osteolysis of chronic GA. In past clinical research, osteolysis has been reported as a clinical characteristic of the severe phase of GA that is tightly regulated by interactions between osteoclasts and osteo-

blasts [15]. The RANK/RANKL pathway plays an important role in osteoclastogenesis, and the RANKL which is secreted by activated T cells and mature osteoblasts is a major factor for osteoclast differentiation [21,24,48]. In this study, confocal images showed that the double-labeling of RANKL- and osteocalcin-positive cells was apparent in the subchondral bone marrow. Thus, the results indicate that RANKL could be expressed by osteoblasts and promote osteoclastogenesis after recurrent MSU injections. However, our micro-CT analysis and histopathological evaluations also proved that the oral administration of etoricoxib could significantly reduce the osteolysis caused by GA. The number of TRAP-positive cells was also significantly reduced after etoricoxib treatment, and confocal images demonstrated that RANKL/osteocalcin-positive cells were obviously reduced after etoricoxib treatment. Therefore, taken together, the results showed that recurrent injections of MSU could mimic the characteristics of human GA with osteolysis but also that NSAIDs, such etoricoxib, are beneficial for the anti-osteoclastogenesis of GA.

In the present study, we used a selective COX-2 inhibitor, etoricoxib, due to its standard use as a clinical drug in GA patients, as a positive control for this rat model. It has been documented that COX-2 played a role in cartilage and bone erosion through the over-production of prostaglandin H₂ (PGH₂) and prostaglandin E₂ (PGE₂). [49]. PGH₂ is the precursor for PGE₂, prostaglandin D₂, prostaglandin F₂, and Thromboxane A₂. The PGE₂-EP4 (PGE₂ receptor) signaling pathways activated through a PGH₂ derivative such as PGE₂ leading to MMPs upregulation induced collagen type II degradation resulting in cartilage degeneration in arthritis [49,50,56,57]. In synovial tissue, COX-2 also contributed to PGH₂ and PGE₂ production and lead to MMPs upregulation through the PGE₂-EP4 pathway [49]. Several studies have indicated that the upregulation of MMPs plays an important role in cartilage degeneration [58]. In the present result, the immunohistochemical staining showed that the protein expression of MMPs and cathepsin k are upregulated after repeat MSU injection and attenuated by etoricoxib treatment. Previous studies demonstrated that MSU could induce inflammatory responses in chondrocyte and fibroblast with upregulating of COX-2 expression [54,55]. From the above evidence, we suggested that etoricoxib could inhibit MMPs upregulation and cartilage degeneration through inhibiting of COX-2 to promote PGH₂ production in GA. Nakata et al. (2018) indicated that the COX-2 activated PGE₂/PGE₂-EP4 pathway resulted in osteoclastogenesis on murine osteocyte of arthritis [49]. Moreover, several studies have found that the COX-2 promoted PGE₂/PGE₂-EP4 pathway could upregulate RANKL expression in osteoblast and promote osteoclast maturation [51–53]. In this study, TRAP and RANKL/osteocalcin positive cells are upregulated after repeated MSU injections and attenuated by etoricoxib. We proposed that etoricoxib attenuated repeat MSU injection-induced bone erosion might be through the inhibition of osteoclastogenesis by RANK/RANKL pathway regulating. We will include the previously mentioned paragraph in the discussion to clarify how etoricoxib is involved in cartilage degeneration and beneficial in anti-osteoclastogenesis.

Conclusion

In conclusion, an investigation of MSU-induced chronic and recurrent attacks of GA in rats was performed in this study. Chronic nociceptive behaviors and chronic inflammatory responses were induced in rats by recurrent intra-articular injections of MSU. Micro-CT and histopathological evaluations further demonstrated joint destruction with osteolysis after recurrent MSU injections. Moreover, MMP-9, MMP-13 and cathepsin K in cartilage and synovial tissue were found to be significantly upregulated by recurrent MSU injections. Meanwhile, it was also found that the oral admin-

istration of an NSAID drug, etoricoxib, could be a useful strategy for inhibiting chronic nociception, chronic inflammation, and cartilage damage via reduced synovial inflammation stemming from reduced MMP-9, MMP-13, and cathepsin K expression after recurrent MSU injections. Moreover, TRAP staining and confocal images demonstrated that recurrent MSU injections induced osteoclastogenesis through osteoblasts expressing RANKL and promoted the RANK/RANKL pathway in this chronic GA model. However, the oral administration of etoricoxib could reduce the expression of TRAP-positive cells and RANKL/osteocalcin-positive cells in subchondral bone marrow. Thus, taken together, the results showed that recurrent injections of MSU could mimic the clinical characteristics of the chronic and severe phase of GA but also that the administration of NSAID drugs, such as etoricoxib, could serve as a useful strategy for decreasing the osteolysis caused by GA. Therefore, we strongly recommend the use of NSAIDs as a useful and beneficial therapeutic strategy for recurrent or chronic GA.

Authors' contributions

Y.Y.L. performed the writing - original draft, methodology and validation. Y.H.J. contributed to writing - original draft and methodology. S.C.L., C.W.F. and N.F.C. contributed to methodology and validation. H.M.K., Y.C.L., T.J.K., H.P.L. contributed to visualization. H.P.L., Z.H.W. directed writing - review & editing and project administration. Authors read and approved the final manuscript.

Compliance with ethic requirements

The use of animals complied with the Guiding Principles in the Care and Use of Animals as approved by the Council of the American Physiology Society and approved by the institutional Animal Care and Use Committee of National Sun Yat-Sen University (approve number: 10424 and 10537).

Declaration of Competing Interest

The authors declare that they have no known competing financial interests or personal relationships that could have appeared to influence the work reported in this paper.

Acknowledgement

This work was supported by the Ministry of Science and Technology of Taiwan (105-2314-B-475-001, 106-2314-B-475-002 and 108-2313-B-110-001 -MY3) and partly supported by Pingtung Christian Hospital (PS104007 & PS105005), Taiwan. And we also thank the Taiwan Animal Consortium (MOST 107-2319-B-001-002) Taiwan Mouse Clinic which is funded by the Ministry of Science and Technology (MOST) of Taiwan for technical support in Micro CT experiment."

Funding

The author(s) received no financial support for the research, authorship, and/or publication of this article.

References

- [1] Underwood M. Gout *BMJ Clin Evid* 2015;2015:1120.
- [2] Ames BN, Cathcart R, Schwiers E, Hochstein P. Uric acid provides an antioxidant defense in humans against oxidant- and radical-caused aging and cancer: a hypothesis. *Proc Natl Acad Sci U S A* 1981;78:6858–62.
- [3] Ragab G, Elshahaly M, Bardin T. Gout: An old disease in new perspective - a review. *J Adv Res* 2017;8:495–511.
- [4] Tausche AK, Richter K, Grassler A, Hansel S, Roch B, Schroder HE. Severe gouty arthritis refractory to anti-inflammatory drugs: treatment with anti-tumour necrosis factor alpha as a new therapeutic option. *Ann Rheum Dis* 2004;63:1351–2.
- [5] Sundry JS, Baraf HS, Yood RA, Edwards NL, Gutierrez-Urena SR, Treadwell EL, et al. Efficacy and tolerability of pegloticase for the treatment of chronic gout in patients refractory to conventional treatment: two randomized controlled trials. *JAMA* 2011;306:711–20.
- [6] Silva CR, Frohlich JK, Oliveira SM, Cabreira TN, Rossato MF, Trevisa G, et al. The antinociceptive and anti-inflammatory effects of the crude extract of *Jatropha isabellei* in a rat gout model. *J Ethnopharmacol* 2013;145:205–13.
- [7] Hoffmeister C, Silva MA, Rossato MF, Trevisan G, Oliveira SM, Zaninelli GP, et al. Participation of the Trpv1 receptor in the development of acute gout attacks. *Rheumatology (Oxford)* 2014;53:240–9.
- [8] Lee HP, Huang SY, Lin YY, Wang HM, Jean YH, Wu SF, et al. Soft coral-derived lemmalol alleviates monosodium urate-induced gouty arthritis in rats by inhibiting leukocyte infiltration and inos, cox-2 and c-fos protein expression. *Mar Drugs* 2013;11:99–113.
- [9] Faires JS, Mccarty D. Acute arthritis in man and dog after intrasynovial injection of sodium urate crystals. *Lancet Oncol* 1962;280:4.
- [10] Fattori V, Zarpelon AC, Staurengo-Ferrari L, Borghi SM, Zaninelli TH, Da Costa FB, et al. Budlein a, a sesquiterpene lactone from *viguiera robusta*, alleviates pain and inflammation in a model of acute gout arthritis in mice. *Front Pharmacol* 2018;9:1076.
- [11] Pineda C, Fuentes-Gomez AJ, Hernandez-Diaz C, Zamudio-Cuevas Y, Fernandez-Torres J, Lopez-Macay A, et al. Animal model of acute gout reproduces the inflammatory and ultrasonographic joint changes of human gout. *Arthritis Res Ther* 2015;17:37.
- [12] Moilanen LJ, Hamalainen M, Lehtimaki L, Nieminen RM, Moilanen E. Urate crystal induced inflammation and joint pain are reduced in transient receptor potential ankyrin 1 deficient mice-potential role for transient receptor potential ankyrin 1 in gout. *PLoS ONE* 2015;10. e0117770.
- [13] Martin WJ, Herst PM, Chia EW, Harper JL. Sesquiterpene dialdehydes inhibit msu crystal-induced superoxide production by infiltrating neutrophils in an in vivo model of gouty inflammation. *Free Radic Biol Med* 2009;47:616–21.
- [14] Dalbeth N, Clark B, Gregory K, Gamble G, Sheehan T, Doyle A, et al. Mechanisms of bone erosion in gout: a quantitative analysis using plain radiography and computed tomography. *Ann Rheum Dis* 2009;68:1290–5.
- [15] McQueen FM, Doyle A, Dalbeth N. Imaging in gout-what can we learn from mri, ct, dect and us?. *Arthritis Res Ther* 2011;13:246.
- [16] Chew N, Cho J. Dual-energy Ct for the diagnosis of sacroiliac and spinal gout. *Joint Bone Spine* 2019;86:259.
- [17] Anne J, Garwood RJ, Lowe T, Withers PJ, Manning PL. Interpreting pathologies in extant and extinct archosaurs using micro-Ct. *PeerJ* 2015;3. e1130.
- [18] Zardi EM, Filippucci E, Navarini L, Afeltra A. Utility of ultrasound in the diagnosis of chronic worsened gout. *J Med Ultrason* 2001;2013(40):467–9.
- [19] Thiele RG. Role of ultrasound and other advanced imaging in the diagnosis and management of gout. *Curr Rheumatol Rep* 2011;13:146–53.
- [20] Baek JM, Kim JY, Yoon KH, Oh J, Lee MS. Ebselen is a potential anti-osteoporosis agent by suppressing receptor activator of nuclear factor kappa-B ligand-induced osteoclast differentiation in vitro and lipopolysaccharide-induced inflammatory bone destruction in vivo. *Int J Biol Sci* 2016;12:478–88.
- [21] Lee SJ, Nam KI, Jin HM, Cho YN, Lee SE, Bone Kim TJ, et al. Destruction by receptor activator of nuclear factor kappaB ligand-expressing T cells in chronic gouty arthritis. *Arthritis Res Ther* 2011;13:R164.
- [22] Lee HP, Lin YY, Duh CY, Huang SY, Wang HM, Wu SF, et al. Lemnalol attenuates mast cell activation and osteoclast activity in a gouty arthritis model. *J Pharm Pharmacol* 2015;67:274–85.
- [23] Seegmiller JE, Howell RR. The old and new concepts of acute gouty arthritis. *Arthritis Rheum* 1962;5:616–23.
- [24] Farrugia AN, Atkins GJ, To LB, Pan B, Horvath N, Kostakis P, et al. Receptor activator of nuclear factor-kappaB ligand expression by human myeloma cells mediates osteoclast formation in vitro and correlates with bone destruction in vivo. *Cancer Res* 2003;63:5438–45.
- [25] Schumacher Jr HR, Boice JA, Daikh DI, Mukhopadhyay S, Malmstrom K, Ng J, et al. Randomised double blind trial of etoricoxib and indometacin in treatment of acute gouty arthritis. *BMJ* 2002;324:1488–92.
- [26] Zhang W, Doherty M, Bardin T, Pascual E, Barskova V, Conaghan P, et al. Eular evidence based recommendations for gout. Part I: Management. Report of a task force of the eular standing committee for international clinical studies including therapeutics (Escisit). *Ann Rheum Dis* 2006;65:1312–24.
- [27] Chaplan SR, Bach FW, Pogrel JW, Chung JM, Yaksh TL. Quantitative assessment of tactile allodynia in the rat paw. *J Neurosci Methods* 1994;53:55–63.
- [28] Hargreaves K, Dubner R, Brown F, Flores C, Joris J. A new and sensitive method for measuring thermal nociception in cutaneous hyperalgesia. *Pain* 1988;32:77–88.
- [29] Jean YH, Chen WF, Duh CY, Huang SY, Hsu CH, Lin CS, et al. Inducible nitric oxide synthase and cyclooxygenase-2 participate in anti-inflammatory and analgesic effects of the natural marine compound lemmalol from formosan soft coral *lemmalia cervicorni*. *Eur J Pharmacol* 2008;578:323–31.
- [30] Lin YC, Huang SY, Jean YH, Chen WF, Sung CS, Kao ES, et al. Intrathecal lemmalol, a natural marine compound obtained from formosan soft coral, attenuates nociceptive responses and the activity of spinal glial cells in neuropathic rats. *Behav Pharmacol* 2011;22:739–50.
- [31] Wen ZH, Tang CC, Chang YC, Huang SY, Lin YY, Hsieh SP, et al. Calcitonin attenuates cartilage degeneration and nociception in an experimental rat model of osteoarthritis: role of Tgf-beta in chondrocytes. *Sci Rep* 2016;6:28862.

- [32] Kao JH, Lin SH, Lai CF, Lin YC, Kong ZL, Wong CS. Shea nut oil triterpene concentrate attenuates knee osteoarthritis development in rats: evidence from knee joint histology. *PLoS ONE* 2016;11(9). e0162022.
- [33] Gerwin N, Bendele AM, Glasson S, Carlson CS. The OARSI histopathology initiative - recommendations for histological assessments of osteoarthritis in the rat. *Osteoarthritis Cartilage* 2010;18(Suppl 3):S24–34.
- [34] Zhang W, Yang N, Shi XM. Regulation of mesenchymal stem cell osteogenic differentiation by glucocorticoid-induced leucine zipper (Gilz). *J Biol Chem* 2008;283:4723–9.
- [35] Hoffmeister C, Trevisan G, Rossato MF, De Oliveira SM, Gomez MV, Ferreira J. Role of Trpv1 in nociception and edema induced by monosodium urate crystals in rats. *Pain* 2011;152:1777–88.
- [36] Modeling Kang C. Gout or gouty (acute) arthritis in biomedical and biochemical infophysics. *WebmedCentral* 2015;WMC004893.
- [37] Dalbeth N, Smith T, Nicolson B, Clark B, Callon K, Naot D, et al. Enhanced osteoclastogenesis in patients with tophaceous gout: urate crystals promote osteoclast development through interactions with stromal cells. *Arthritis Rheum* 2008;58:1854–65.
- [38] Getting SJ, Flower RJ, Parente L, De Medicis R, Lussier A, Wolitzky BA, et al. Molecular determinants of monosodium urate crystal-induced murine peritonitis: a role for endogenous mast cells and a distinct requirement for endothelial-derived selectins. *J Pharmacol Exp Ther* 1997;283:123–30.
- [39] Nissinen L, Kahari VM. Matrix metalloproteinases in inflammation. *Biochim Biophys Acta* 2014;1840:2571–80.
- [40] Hao L, Zhu G, Lu Y, Wang M, Jules J, Zhou X, et al. Deficiency of cathepsin K prevents inflammation and bone erosion in rheumatoid arthritis and periodontitis and reveals its shared osteoimmune role. *FEBS Lett* 2015;589:1331–9.
- [41] Ben-Chetrit E, Bergmann S, Sood R. Mechanism of the anti-inflammatory effect of colchicine in rheumatic diseases: a possible new outlook through microarray analysis. *Rheumatology (Oxford)* 2006;45:274–82.
- [42] Qaseem A, Harris RP, Forciea MA. Clinical guidelines committee of the American college of P. management of acute and recurrent gout: a clinical practice guideline from the American college of physicians. *Ann Intern Med* 2017;166:58–68.
- [43] Zhang S, Zhang Y, Liu P, Zhang W, Ma JL, Wang J. Efficacy and safety of etoricoxib compared with nsaid in acute gout: a systematic review and a meta-analysis. *Clin Rheumatol* 2016;35:151–8.
- [44] Muehleman C, Li J, Aigner T, Rappoport L, Mattson E, Hirschmugl C, et al. Association between crystals and cartilage degeneration in the ankle. *J Rheumatol* 2008;35:1108–17.
- [45] McQueen FM, Chhana A, Dalbeth N. Mechanisms of joint damage in gout: evidence from cellular and imaging studies. *Nat Rev Rheumatol* 2012;8:173–81.
- [46] Girish G, Melville DM, Kaeley GS, Brandon CJ, Goyal JR, Jacobson JA, et al. Imaging appearances in gout. *Arthritis* 2013;2013. 673401.
- [47] Eriksen EF. Treatment of bone marrow lesions (bone marrow edema). *Bonekey Rep* 2015;4:755.
- [48] Boyce BF, Xing L. Biology of rank, rankl, and osteoprotegerin. *Arthritis Res Ther* 2007;9(Suppl 1):S1.
- [49] Nakata K, Hanai T, Take Y, Osada T, Tsuchiya T, Shima D, et al. Disease-modifying effects of COX-2 selective inhibitors and non-selective NSAIDs in osteoarthritis: a systematic review. *Osteoarthritis Cartilage* 2018;26:1263–73.
- [50] Chen SH, Fahmi H, Shi Q, Benderdour M. Regulation of microsomal prostaglandin E2 synthase-1 and 5-lipoxygenase-activating protein/5-lipoxygenase by 4-hydroxynonenal in human osteoarthritic chondrocytes. *Arthritis Res Ther* 2010;12:R21.
- [51] Peng YJ, Lee CH, Wang CC, Salter DM, Lee HS. Pycnogenol attenuates the inflammatory and nitrosative stress on joint inflammation induced by urate crystals. *Free Radic Biol Med* 2012;52:765–74.
- [52] Nam JS, Jagga S, Sharma AR, Lee JH, Park JB, Jung JS, et al. Anti-inflammatory effects of traditional mixed extract of medicinal herbs (MEMH) on monosodium urate crystal-induced gouty arthritis. *Chin J Nat Med* 2017;15:561–75.
- [53] Ohshiba T, Miyaura C, Ito A. Role of prostaglandin E produced by osteoblasts in osteolysis due to bone metastasis. *Biochem Biophys Res Commun* 2003;300:957–64.
- [54] Park HJ, Baek K, Baek JH, Kim HR. TNFalpha increases RANKL expression via PGE(2)-induced activation of NFATc1. *Int J Mol Sci* 2017;18(3).
- [55] Suda K, Udagawa N, Sato N, Takami M, Itoh K, Woo JT, et al. Suppression of osteoprotegerin expression by prostaglandin E2 is crucially involved in lipopolysaccharide-induced osteoclast formation. *J Immunol* 2004;172:2504–10.
- [56] Su SC, Tanimoto K, Tanne Y, Kunimatsu R, Hirose N, Mitsuyoshi T, et al. Celecoxib exerts protective effects on extracellular matrix metabolism of mandibular condylar chondrocytes under excessive mechanical stress. *Osteoarthritis Cartilage* 2014;22:845–51.
- [57] Attur M, Al-Mussawir HE, Patel J, Kitay A, Dave M, Palmer G, et al. Prostaglandin E2 exerts catabolic effects in osteoarthritis cartilage: evidence for signaling via the EP4 receptor. *J Immunol* 2008;181(7):5082–8.
- [58] Tateiwa D, Yoshikawa H, Kaito T. Cartilage and Bone Destruction in Arthritis: Pathogenesis and Treatment Strategy: A Literature Review. *Cells* 2019;8(8).